Journal of King Saud University – Science 35 (2023) 102836

HOSTED BY

Contents lists available at ScienceDirect

Journal of King Saud University – Science

journal homepage: www.sciencedirect.com

Original article

Structural, optical and thermoelectric properties of (Al and Zn) doped Co_9S_8-NPs synthesized via co-precipitation method

Tariq Munir [a], Arslan Mahmood [a,*], Shafaq Fatima [a], Amjad Sohail [a], Muhammad Fakhar-e-Alam [a], Muhammad Atif [b], Noman Rafaqat [c,*]

[a] Department of Physics, Government College University Faisalabad (GCUF), Allama Iqbal Road, Faisalabad 38000, Pakistan
[b] Department of Physics and Astronomy, College of Science, King Saud University Riyadh 11451, Saudi Arabia
[c] Institute of Photonics, University of Eastern Finland, Yliopistokatu 7, 80100 Joensuu, Finland

ARTICLE INFO

Article history:
Received 27 March 2023
Revised 31 May 2023
Accepted 1 August 2023
Available online 9 August 2023

Keywords:
Cobalt sulfide
Agglomeration
Band gap
Thermoelectric material
Energy storage devices

ABSTRACT

In the previous decade nanostructure materials have emerged as the necessary ingredient in electronic application and enhancement of device performance. Cobalt sulfide is one such transition metal sulfide which has provoked a lot of interest in the field of research. The present study was related to pure, (Al and Zn) doped cobalt sulfide NPs have been fabricated using facile co-precipitation method. The cubic structure has conformed to XRD analysis and crystallite size of pure and doped Co_9S_8 NPs in the range of 11 to 29 nm and with W-H method varies from 29 to 51 nm. The SEM micrograph shows that the agglomeration of the particles in the form of clusters. To conform the vibrational modes of (Al and Zn) doped Co_9S_8-NPs was done with Raman spectroscopy analysis. The absorbance of prepared materials was investigated with UV–VIS and it was also observed that the band gap decreased from 3.6 to 1.94 eV with doping agents. In case of IV analysis shows that the resistivity decreased and conductivity increased of Al and Zn doped Co_9S_8 NPs. Furthermore, the sharp increase in potential difference at lower temperature indicates that the doped material is an excellent thermoelectric material for energy storage devices.

1. Introduction

Nanotechnology has the ability and potential to give us cleaner, cheaper and more productive methods to create new energy sources (Li et al., 2019). This can facilitate developing countries to solve their energy scarcity problems and create self-sufficiency. Thus nanotechnology will prove to be a solution which will solve many of our problems and become a handy tool. The development of innovative material in this regard can pave way for new applications. Thus it can revolutionize the whole energy sector (Chen et al., 2012; Mahmood et al., 2022). In this regard metal sulfides have drawn great scientific interest (Shi et al., 2012; Munir et al., 2023a, 2023b). Many studies have been done on metal sulfides because of their vast potential (Thangasamy et al., 2020). Many investigations have shown that metal sulfides are much attractive alternative than metal oxides and hydroxides (Jeevanandam et al., 2018). Metal oxides are being used as pseudo capacitors materials presented a review on nickel cobalt sulfide (Munir et al., 2023a, 2023b). They elucidated the fact that it was need of the day to look for substitutes of fossil fuels deposited a layer of cobalt sulfide on reduced graphene oxide through a hydrothermal method to prepare a high capacity material.

From the metal sulfides studies cobalt sulfide has emerged as a very attractive candidate for electrode materials and it can also be used in solar cells (Zhu et al., 2020). The previous study provided the information about prepared Ni-doped copper cobalt sulfide NPs for use in hydrogen evolution reaction. Furthermore, various properties of copper doped cobalt sulfide particles and found that the material was a suitable option for photocatalytic activity (Munir et al., 2020). Synthesized β-cobalt sulfide NPs and deposited them on graphene to prepare super-capacitor. However applications of some of these sulfides is confined due to rapid capacity fading and degeneration during cycling which eventually results in disconnection between electrodes.

Therefore these sulphide base metals can be used in conjunction with other materials was preferred a catalyst in

* Corresponding authors.
E-mail addresses: arslan4physics@gmail.com (A. Mahmood), nrafaqat@uef.fi (N. Rafaqat).
Peer review under responsibility of King Saud University

Production and hosting by Elsevier

https://doi.org/10.1016/j.jksus.2023.102836
1018-3647/

oxygen evolution reaction (Akram et al., 2020). The anode or cathode material in supercapacitors was fabricated (Bian et al., 2020) and sodium and lithium batteries were reported Han et al. (2017a, 2017b). Nowadays a lot of research is being done to explore potential materials for use in nanotechnology. As these materials can be used to tailor a specific material and study its optical, structural and thermoelectric properties. Various physical parameters can be improved by selecting a suitable material. Transition metals are being extensively used for doping because of their particular electronic configuration as doping brings about a drastic change in its various characteristics (Munir et al., 2022). Cobalt sulphide is gaining increasing importance because of its excellent use in many applications (DeCarlo and Matthews, 2019). Many physical parameters of transition metal doped cobalt sulphide may be improved by engineering new alloys. In the present study Al and Zn doped cobalt sulphide and investigate its various properties was studied by using different characterization techniques.

2. Experimental

2.1. Materials

The pure and doped Co_9S_8-NPs was synthesized by using various precursor such as cobalt chloride ($CoCl_2{\cdot}H_2O$), sodium sulfide (Na_2S), zinc chloride ($ZnCl_2$), aluminum chloride ($AlCl_3$), ethanol (C_2H_5OH) and de-ionized water.

2.2. Preparation of materials

The cobalt chloride solution was put in a beaker and placed on a magnetic stirrer while keeping the temperature at 80 °C till a uniform solution was obtained. The sodium sulfide solution was then added from a burette drop wise with constant stirring. Then 4 to 5 drops of ammonia solution were added until the solution obtained a pH of 7. The resulting solution was then heated with constant stirring for 30 min until it attained a temperature of 75 °C.The solution thus prepared was kept without any interference for 24 h until solid precipitates settled at the bottom of the breaker. The clear liquid obtained at the surface was then drained and the resulting precipitates were them filtered by a filter paper and collected in petri dishes. The filtered sample thus obtained was placed in an oven and dried at 200 °C. They were then dried at suitable conditions for 24 h. The precipitates were then transferred to a mortar and pestle and the sample were then grinded into a very fine powder. Later these nanoparticles were characterized.

2.3. Material characterization techniques

The XRD with specification BRUKER D8 ADVANCED (Cu_α "1.54-nm") was used to investigate the defects in crystal and also used to identify the phase of nanomaterials. The cube emcraft SEM examine the surface morphology and the Raman spectroscopy "MN STEX-PRI 100" was identified the Raman spectra. Optical behavior of Co_9S_8 NPs was calculated with "PerkinElmer" and the electrical resistivity and conductivity was observed with two probe method. Finally, the thermoelectric properties were investigated the pure, Al and Zn doped Co_9S_8 NPs with seebeck coefficient.

3. Results and discussion

3.1. XRD analysis

X-ray diffraction was employed to study the structural parameters of undoped, Zn and Al doped cobalt sulfide NPs. The spectrum was scanned at an angle of 2θ between 20° to 80°. Fig. 1 shows the

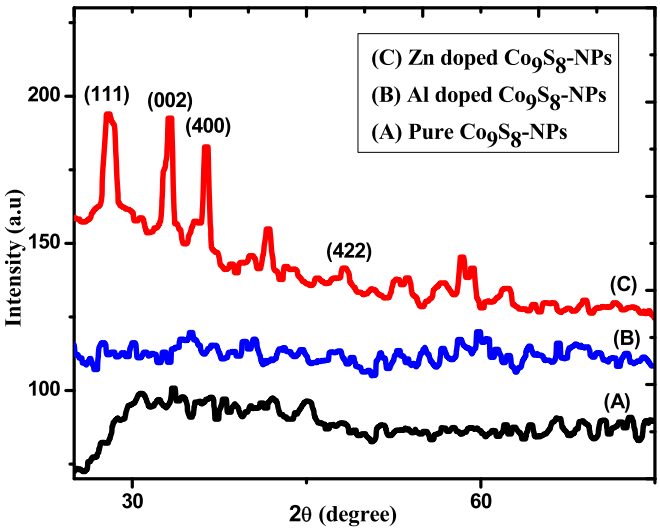

Fig. 1. XRD spectra of pure, Al and Zn doped Co_9S_8-NPs.

diffraction planes (222), (400), (420), (422) corresponding to diffraction angles of 31.37°, 36.50°, 41.45° and 44.81° (Muradov et al., 2018). The value of lattice constant came out to be 9.4 A° which agreed with the values have been reported in previous papers (Munir et al., 2020; Muradov et al., 2018). These planes described the cubic structure of Co_9S_8 which is in the space group of Fm3m. Some new peaks were observed with the doping of zinc which were seen at (111), (002), (400) and (101) at angles of 28.35°, 33.29°, 36.15° and 43° respectively, which were in good agreement from the literature (Ullah et al., 2011). The peak which has been observed between 33° to 36° is pointing to cobalt sulfide phase as observed in previous reported data (Kumar et al., 2014). XRD results for aluminum doped cobalt sulfide show peaks obtained at 35.36°, 40.93°, 60.17° and 76.12° which corresponds to planes (400), (200), (220) and (311) respectively and it was confirmed from literature (Ayieko et al., 2015). These new peaks confirmed the presence of aluminum in the cobalt sulfide structure. The Table 1 shows that there has been an increase in the crystallite size after doping with Zn and Al.

$$D = \frac{k\lambda}{\beta cos\theta} \quad (1)$$

The above equation *D* represents crystallite size, shape factor is denoted by *K* which has a value of 0.94, β is the acronym for full width at half maxima. The wavelength of the incident radiation was given by λ which is 0.15406 nm.

The imperfection in crystal was investigated by W-H method and variation in crystallite size depends upon the diffracting domain and polycrystalline nature of nanomaterials. The lattice strain of Co_9S_8NPs (0.0045), Al doped Co_9S_8NPs (0.0046) and Zn doped Co_9S_8 NPs (0.0014). The variation in lattice strain which cause the presence of defects in undoped and doped Co_9S_8 NPs. The scherrer equation was preferred to calculate the crystallite size and the instrumental error occurrence in peak broadening (Liu

Table 1
Comparison of crystallite size for pure and doped cobalt sulfide.

NPs	$D_{scherrer}$ (nm)	$D_{W\text{-}H}$ (nm)
Co_9S_8 NPs	11.6	29
Zn doped Co_9S_8 NPs	28.8	51
Al doped Co_9S_8 NPs	15	46

et al., 2017; Munir et al., 2021) The peak broadening level can be reducing via W-H technique.

$$\beta cos\theta = \frac{k\lambda}{D} + 4\varepsilon sin\theta \quad (2)$$

The equation (I) and (II) was used to calculate the crystallite size via Scherrer and W-H methods. The Fig. 2 represents plot a graph between $\beta cos\theta$ and 4 $sin\theta$ and the slope of linear fitting curve was calculated. The variation in crystallite size due to internal stress of undoped, Al and Zn doped Co_9S_8-NPs. The microstrains in nanomaterial were removed by scherrer equation and ignore the peak broadening via W-H method (Iqbal et al., 2020).

3.2. SEM analysis

The SEM was employed to assess the surface morphology of undoped, Zn and Al doped Cobalt sulfide NPs. Fig. 3(a) displays the results for pure cobalt sulfide NPs and it was depicted the grain like structure. The Fig. 3(b) and (c) shows that the Zn and Al doped cobalt sulfide NPs. It was observed that particles had agglomerated groups of nanoparticles which were spherical, non-uniform and irregular surface. The previous results show that due to decrease lattice constant after doping agents, which could be attributed to the fact that both Zn and Al have a smaller diameter.

3.3. Optical analysis

The UV–visible spectroscopy was employed to measure the energy band gap in pure cobalt sulfide and when it was doped with zinc (Zn) and aluminum (Al).

The above Fig. 4 shows that the graph which has been plotted between absorbance and wavelength for pure and doped cobalt sulfide NPs. It can be seen that doped cobalt sulfide shows more absorption of light in comparison with pure cobalt sulfide NPs. It was also observed that the absorbance edge is slightly shifted towards longer wavelength which ascertains the incorporation of dopant element in Co_9S_8 NPs. The absorption bands between 300 nm and 400 nm can be attributed to the metal sulfide nanoparticles.

The Fig. 5 shows energy gap E_g for undoped, Al and Zn doped cobalt sulfide is found out by adopting Tauc formula expressed in Eq. (2). This formula is based on the principle that intensity of the optical absorption is found by calculating the difference in the energy of photon and band gap.

$$(\alpha hv)^{\frac{1}{n}} = A(hv - E_g) \quad (3)$$

α, Represents absorption co-efficient, "A" is constant, "hv" is the energy of photon and E_g is the difference of energy between valance band and conduction band (Ahmad et al., 2021).

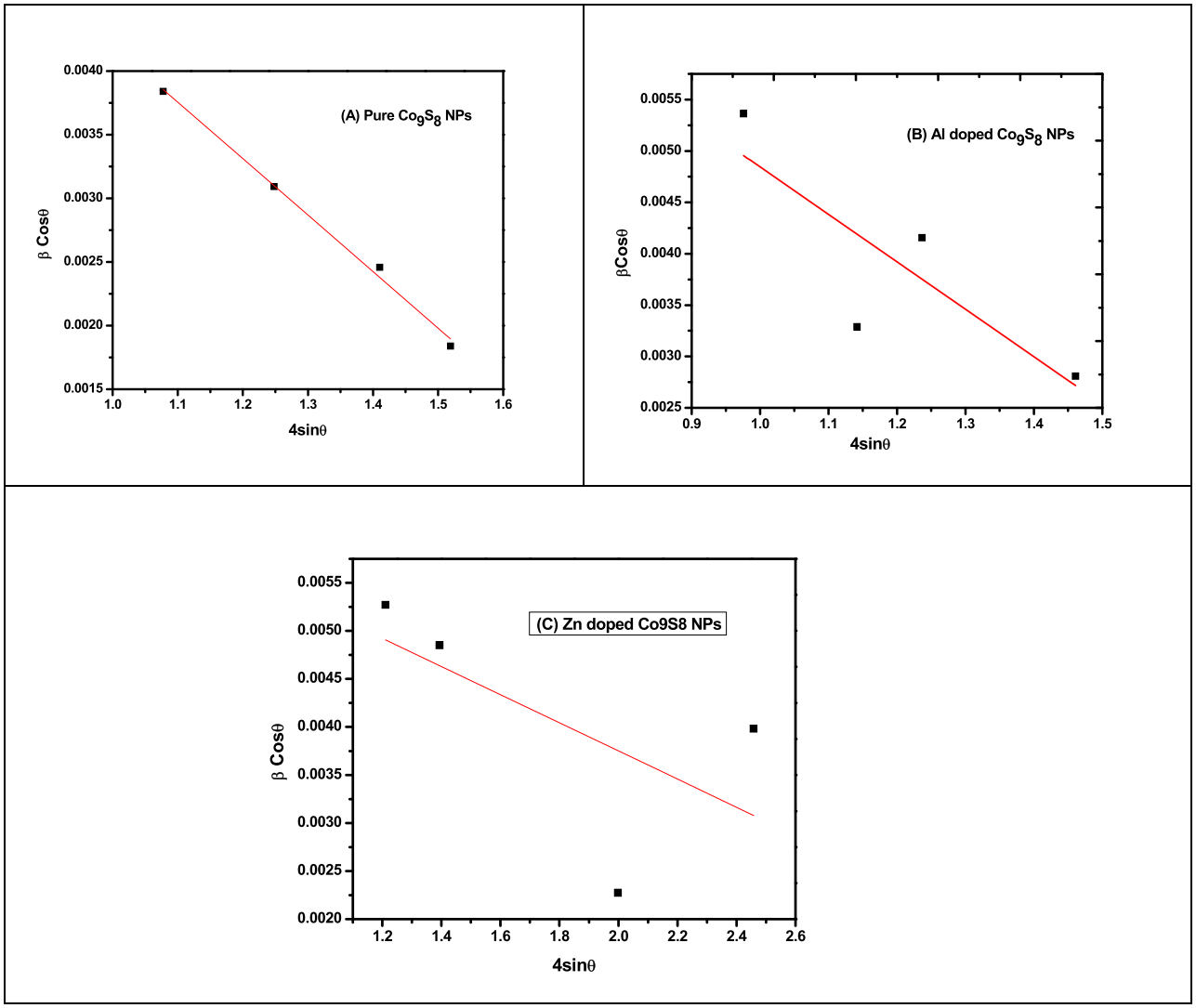

Fig. 2. W-H plot of undoped, Al and Zn doped Co_9S_8 NPs.

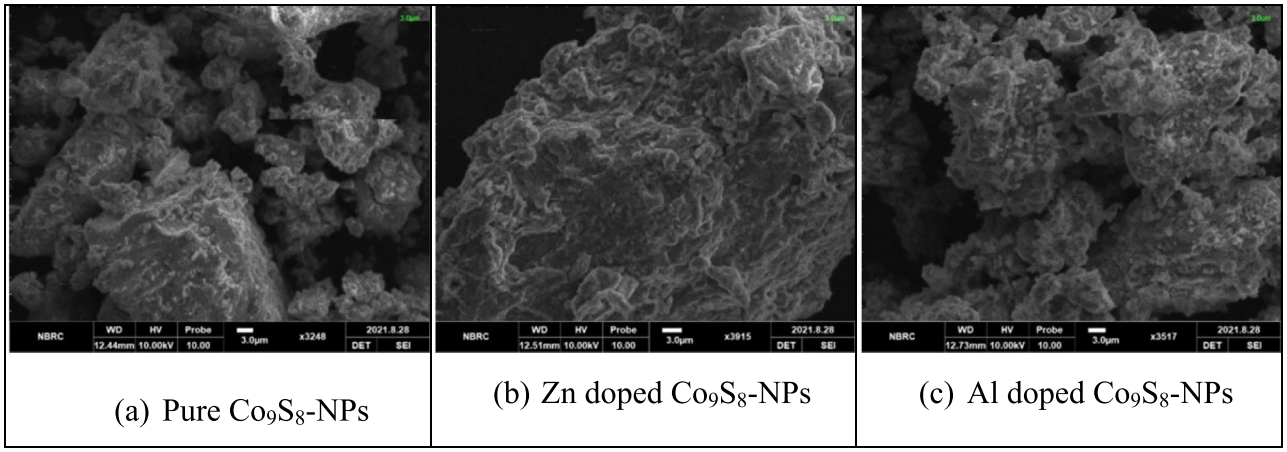

Fig. 3. Shows SEM micrograph of pure, Zn and Al doped cobalt sulfide NPs.

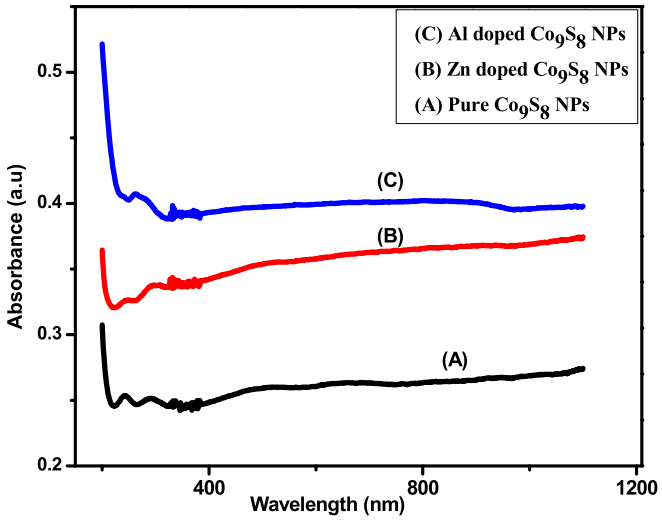

Fig. 4. Absorption spectra for pure, Zn and Al doped cobalt sulfide NPs.

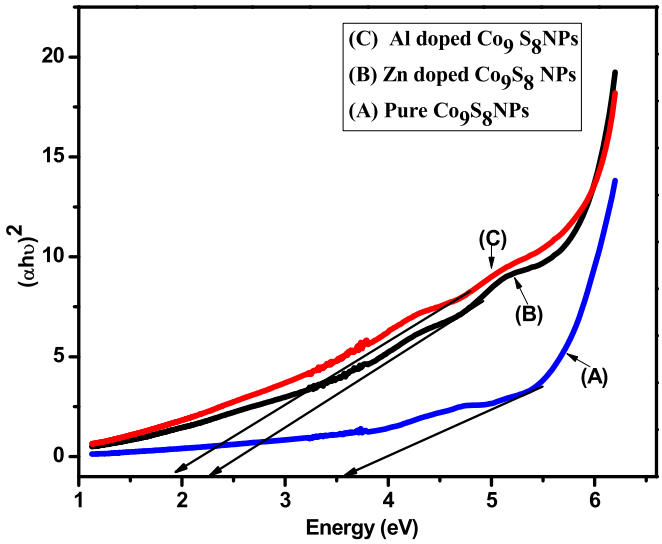

Fig. 5. Tauc plot of pure, Zn and Al doped cobalt sulfide NPs.

To compare the value of band gap a graph was drawn between $(\alpha h\nu)^2$ and energy (eV). These values are given in Table 2 below.

It can be seen that with doping elements the band gap has been decreased significantly and the nature of material is useful for photo-catalytic activity purpose.

3.4. Raman spectroscopy analysis

Raman spectroscopy was used to investigate the vibrational modes in cobalt sulfide nanoparticles. In this work, Raman spectroscopy confocal micro Raman mapping system, with laser wavelength 633 nm, has been used to study synthesized aluminum and zinc doped cobalt sulfide.

The Fig. 6 shows that the peaks at 460 cm^{-1} and 670 cm^{-1} could be associated to Co_9S_8 in all the three samples as studied by Xie et al., (2019) and the peaks at 1000 cm^{-1} can be attributed to a metal composite.

3.5. I-V analysis

The electrical behavior of undoped, Al and Zn doped Co_9S_8 NPs were examined by two probe method. Fig. 7 indicated that he resistivity and conductivity of Co_9S_8 NPs varies with doping Zn and Al. The resistivity of Co_9S_8 NPs decreased with Al and Zn doping agents and conductivity of Co_9S_8NPs increased with the same doping agents. Due to increase the conductivity and decrease resistivity of doped Co_9S_8 NPs compared with ITO (indium tin oxide). The Al and Zn doped Co9S8 NPs are most suitable for electrical, optical and photoelectric properties.

3.6. Seebeck analysis

To find the seebeck coefficient a graph was plotted between temperatures and generated potential difference of pure Co_9S_8 NPs. It was observed that there was a sharp increase in the potential difference after a temperature of 40 °C. The slope of the graph

Table 2
Bandgap values of pure and doped cobalt sulfide NPs.

Nanoparticles	Bandgap value (eV)
Pure Co_9S_8 NPs	3.6
Zn doped Co_9S_8 NPs	2.32
Al doped Co_9S_8 NPs	1.94

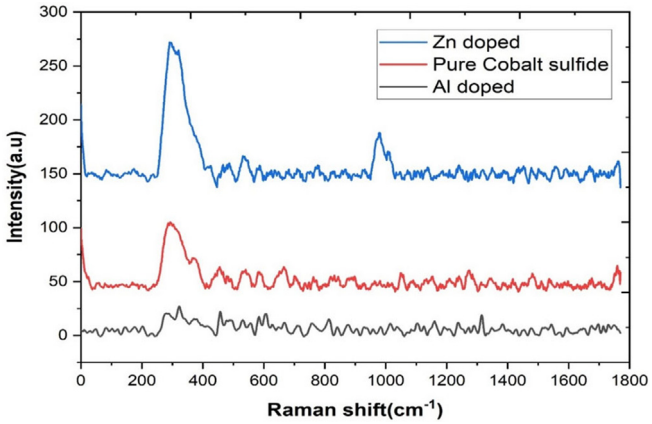

Fig. 6. Raman spectra of Co_9S_8 and Aluminum and Zinc doped Cobalt sulfide.

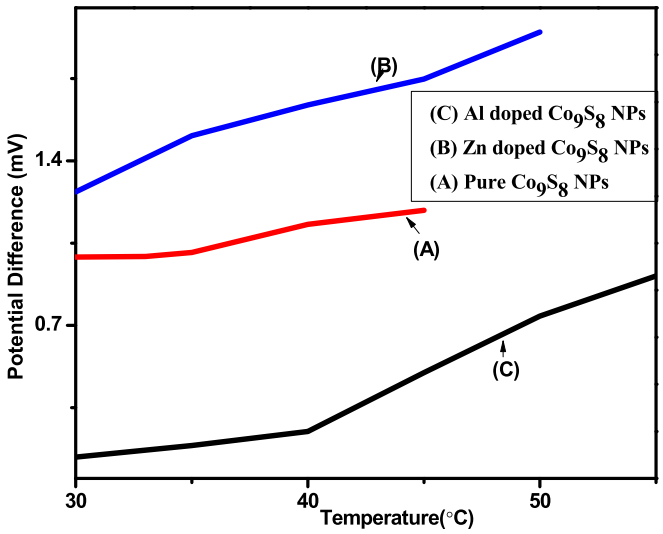

Fig. 8. Thermoelectric behavior of Pure, Al and Zn doped Co_9S_8 -NPs.

came out to be 0.022. The Fig. 8 shows that the graph was plotted between the temperatures and generated potential difference of Zn doped cobalt sulfide there was a sharp increase in the generated potential difference after 34 °C. The slope of the graph was found to be 0.024 which was more than that of pure cobalt sulfide NPs. Furthermore, again the graph was plotted between temperature and potential difference of Al doped Co_9S_8 NPs, it was found that the generated potential started increasing immediately after 30 °C. Whereas the temperature at which the potential started increasing was 40 °C in pure cobalt sulfide and 34 °C in zinc doped cobalt sulfide NPs. The slope of the graph when calculated was found to be 0.025 which was also larger than both zinc doped and pure cobalt sulfide particles (Fig. 8). It is observed that with the increase of temperature there was an exponential increase in current which shows that carriers acquire more thermal energy which gives them and increased kinetic energy. This gives them increased mobility which causes sudden increase in current. This behavior leads us to consider that aluminum doped cobalt sulfide particles show greater efficiency for use as thermoelectric material.

4. Conclusion

The XRD pattern of the undoped and doped cobalt sulfide confirmed the nanocrystalline cubic structure. SEM analysis revealed that some of the particles were found to be very fine. The doping increased the agglomeration of the particles and they were found to be mostly spherical in shape and grouped together in the form of clusters. It was observed that the band-gap value decreased from 3.6 eV to 1.94 eV upon doping showing that the materials were suitable for photocatalytic activity. It was found that as the temperature of the sample was increased there was an increase in the potential generated in the nanoparticles. The slope of the graphs plotted between the temperature and the potential difference was found to have increased more in aluminum than in zinc

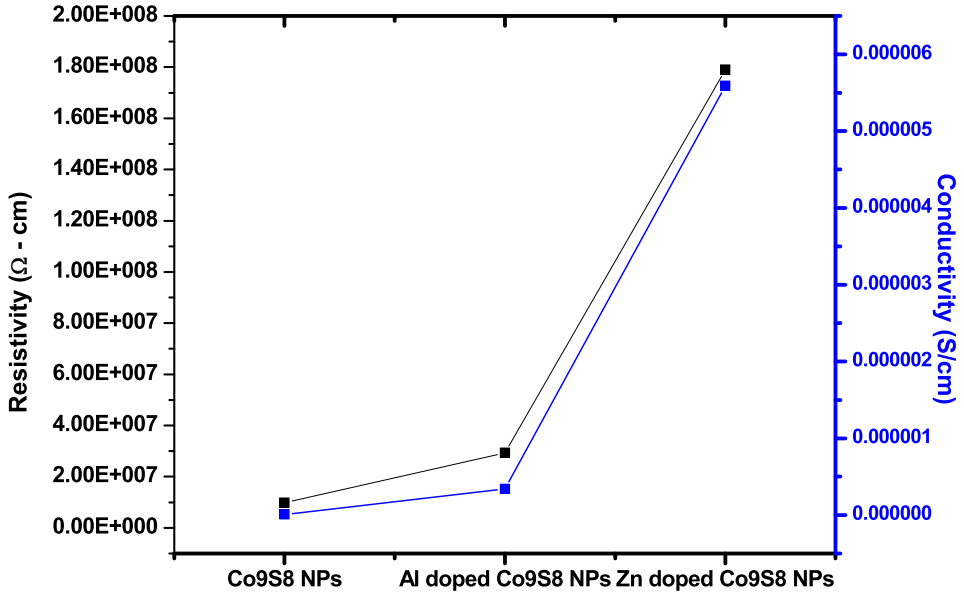

Fig. 7. Resistivity and conductivity of Al and Zn doped Co_9S_8 NPs.

and pure cobalt sulfide. Therefore it can be concluded that cobalt sulfide doped with zinc and aluminum was found to be a good thermoelectric material as the temperature for which the potential difference increased was found to have decreased with the doping. The overall assessment shows that metal doped Co9S8 NPs are most suitable for thermoelectric properties.

Declaration of Competing Interest

The authors declare that they have no known competing financial interests or personal relationships that could have appeared to influence the work reported in this paper.

Acknowledgement

Researchers Supporting Project number (RSP2023R397), King Saud University, Riyadh, Saudi Arabia

Appendix A. Supplementary material

Supplementary data to this article can be found online at https://doi.org/10.1016/j.jksus.2023.102836.

References

Ahmad, D., Khan, M.A., Mahmood, A., Sohail, A., Gillani, S.A., 2021. Structural and optical properties of molybdenum oxide thin films prepared by the dip coating technique. Eur. Phys. J. Appl. Phys. 93 (3), 30301.

Akram, R., Khan, M.D., Zequine, C., Zhao, C., Gupta, R.K., Akhtar, M., Bhatti, M.H., 2020. Cobalt sulfide nanoparticles: synthesis, water splitting and supercapacitance studies. Mater. Sci. Semicond. Process. 109, 104925.

Ayieko, C.O., Musembi, R.J., Ogacho, A.A., Aduda, B.O., Muthoka, B.M., & Jain, P.K., 2015. Controlled texturing of aluminum sheet for solar energy applications.

Bian, R., Song, D., Si, W., Zhang, T., Zhang, Y., Lu, P., Liang, J., 2020. Carbon nanotubes@ nickel cobalt sulfide nanosheets for high-performance supercapacitors. ChemElectroChem 7 (17), 3663–3669.

Chen, Z.G., Han, G., Yang, L., Cheng, L., Zou, J., 2012. Nanostructured thermoelectric materials: current research and future challenge. Prog. Nat. Sci.: Mater. Int. 22 (6), 535–549.

DeCarlo, S., Matthews, D., 2019. More than a pretty color: the renaissance of the cobalt industry. J. Int'l Com. & Econ. 1.

Han, F., Tan, C.Y.J., Gao, Z., 2017a. Template-free formation of carbon nanotube-supported cobalt sulfide@ carbon hollow nanoparticles for stable and fast sodium ion storage. J. Power Sources 339, 41–50.

Han, F., Zhang, C., Sun, B., Tang, W., Yang, J., Li, X., 2017b. Dual-carbon phase-protective cobalt sulfide nanoparticles with cable-type and mesoporous nanostructure for enhanced cycling stability in sodium and lithium ion batteries. Carbon 118, 731–742.

Iqbal, S., Shaid, N.A., Sajid, M.M., Javed, Y., Fakhar-e-Alam, M., Mahmood, A., Sarwar, M., 2020. Extensive evaluation of changes in structural, chemical and thermal properties of copper sulfide nanoparticles at different calcination temperature. J. Cryst. Growth 547, 125823.

Jeevanandam, J., Barhoum, A., Chan, Y.S., Dufresne, A., Danquah, M.K., 2018. Review on nanoparticles and nanostructured materials: history, sources, toxicity and regulations. Beilstein J. Nanotechnol. 9 (1), 1050–1074.

Kumar, N., Raman, N., Sundaresan, A., 2014. Synthesis and properties of cobalt sulfide phases: CoS_2 and Co_9S_8. Zeitschriftfüranorganische und allgemeineChemie 640 (6), 1069–1074.

Li, H., Li, Z., Sun, M., Wu, Z., Shen, W., Fu, Y.Q., 2019. Zinc cobalt sulfide nanoparticles as high performance electrode material for asymmetric supercapacitor. ElectrochimicaActa 319, 716–726.

Liu, X., Li, Q., Zhao, Y., Dong, Y., Fan, Q., Kuang, Q., 2017. A promising mechanical ball-milling method to synthesize carbon-coated Co 9 S 8 nanoparticles as high-performance electrode for supercapacitor. J. Mater. Sci. 52, 13552–13560.

Mahmood, A., Munir, T., Fakhar-e-Alam, M., Atif, M., Shahzad, K., Alimgeer, K.S., Ahmad, S., 2022. Analyses of structural and electrical properties of aluminium doped ZnO-NPs by experimental and mathematical approaches. J. King Saud Univ.-Sci. 34, (2), 101796.

Munir, T., ur Rehman, N., Mahmood, A., Mahmood, K., Ali, A., Khan, I., Manzoor, A., 2020. Structural, optical, electrical and thermo-electrical properties of Cu doped Co_9S_8-NPs synthesized via co-precipitation method. Chem. Phys. Lett. 761, 137989.

Munir, T., Mahmood, A., Ahmad, N., Atif, M., Alimgeer, K.S., Fatehmulla, A., Ahmad, H., 2021. Structural, electrical and optical properties of Zn1− xCuxO (x= 0.00–0.09) nanoparticles. J. King Saud Univ.-Sci. 33, (2), 101330.

Munir, T., Imran, M., Muzammil, S., Hussain, A.A., Alam, M.F.E., Mahmood, A., Afzal, M., 2022. Antimicrobial activities of polyethylene glycol and citric acid coated graphene oxide-NPs synthesized via Hummer's method. Arab. J. Chem. 15, (9), 104075.

Munir, T., Mahmood, A., Peter, N., Rafaqat, N., Imran, M., Ali, H.E., 2023a. Structural, morphological and optical properties at various concentration of Ag doped SiO_2-NPs via sol gel method for antibacterial and anticancer activities. Surf. Interfaces 38, 102759.

Munir, T., Mahmood, A., Rasul, A., Imran, M., Fakhar-e-Alam, M., 2023b. Biocompatible polymer functionalized magnetic nanoparticles for antimicrobial and anticancer activities. Mater. Chem. Phys. 301, 127677.

Muradov, M.B., Balayeva, O.O., Azizov, A.A., Maharramov, A.M., Qahramanli, L.R., Eyvazova, G.M., Aghamaliyev, Z.A., 2018. Synthesis and characterization of cobalt sulfide nanoparticles by sonochemical method. Infrared Phys. Technol. 89, 255–262.

Shi, W., Zhu, J., Rui, X., Cao, X., Chen, C., Zhang, H., Yan, Q., 2012. Controlled synthesis of carbon-coated cobalt sulfide nanostructures in oil phase with enhanced Li storage performances. ACS Appl. Mater. Interfaces 4 (6), 2999–3006.

Thangasamy, P., Oh, S., Nam, S., Randriamahazaka, H., Oh, I.K., 2020. Ferrocene-incorporated cobalt sulfide nanoarchitecture for superior oxygen evolution reaction. Small 16 (31), 2001665.

Ullah, S., Amin Badshah, F.A., Raza, R., Altaf, A.A., Hussain, R., 2011. Electrodeposited zinc electrodes for high current Zn/AgO bipolar batteries.

Xie, B., Yu, M., Lu, L., Feng, H., Yang, Y., Chen, Y., Liu, J., 2019. Pseudocapacitive Co_9S_8/graphene electrode for high-rate hybrid supercapacitors. Carbon 141, 134–142.

Zhu, Y., Li, J., Yun, X., Zhao, G., Ge, P., Zou, G., Ji, X., 2020. Graphitic carbon quantum dots modified nickel cobalt sulfide as cathode materials for alkaline aqueous batteries. Nano-Micro Lett. 12 (1), 1–18.